Dynamical Mean Field Theory with the Density Matrix Renormalization Group

Daniel J. García,[1] Karen Hallberg,[1] and Marcelo J. Rozenberg[2,3]

[1]*Instituto Balseiro and Centro Atómico Bariloche, 8400 Bariloche, Argentina*
[2]*Laboratoire de Physique des Solides, UMR8502, Université Paris-Sud, 91405 Orsay, France*
[3]*Departamento de Física, FCEN, Universidad de Buenos Aires, Buenos Aires (1428), Argentina*

(Received 4 March 2004; published 7 December 2004)

A new numerical method for the solution of the dynamical mean field theory's self-consistent equations is introduced. The method uses the density matrix renormalization group technique to solve the associated impurity problem. The new algorithm makes no *a priori* approximations and is only limited by the number of sites that can be considered. We obtain accurate estimates of the critical values of the metal-insulator transitions and provide evidence of substructure in the Hubbard bands of the correlated metal. With this algorithm, more complex models having a larger number of degrees of freedom can be considered and finite-size effects can be minimized.

DOI: 10.1103/PhysRevLett.93.246403 PACS numbers: 71.10.Fd, 71.27.+a, 71.30.+h

Great theoretical progress in our understanding of the physics of strongly correlated electron systems has been possible since the introduction of the dynamical mean field theory (DMFT) [1,2]. It has allowed the successful investigation of model Hamiltonians relevant for problems as diverse as colossal magneto-resistance, heavy fermions, metal-insulator transitions (MI), etc. [3]. Presently, the field of realistic band-structure calculations of strongly correlated systems in which density functional theory is blended with DMFT is undergoing a burst of activity as was highlighted by Kotliar and Vollhardt [4]. In that approach, DMFT is the local correlation physics "engine" that brings in the many-body effects lacking in *ab-initio* methods [5,6]. In addition, unlike earlier approaches [7], in DMFT, no approximations are made on the dynamics; therefore, one obtains detailed information on distribution and transfers of spectral weights that are relevant for the interpretation of experiments such as photoemission, optical conductivity, and scanning tunneling microscopy. A successful and reliable theory of real strongly correlated materials is one of the current main challenges in condensed matter physics.

At the heart of the DMFT method is the solution of an associated quantum impurity model where the environment of the impurity has to be determined self-consistently. Therefore, the ability to obtain reliable DMFT solutions of lattice model Hamiltonians relies directly on the ability to solve quantum impurity models. Since solutions of general impurity models are usually not analytically tractable, one has to resort to numerical algorithms or approximate methods. Among the *a priori* exact numerical algorithms available we count the Hirsch-Fye Quantum Monte Carlo [8] method and Wilson's numerical renormalization group (NRG) [9]. The former is a finite-temperature method that is formulated in imaginary time and has been applied to a large variety of impurity models including the multiorbital case that corresponds to correlated multiband lattice Hamiltonians [10]. While this method is very stable and accurate and allowed for detailed investigations of fundamental problems such as the metal-insulator transition in the Hubbard model [3,11], its main drawback is that the access to real frequency quantities such as spectral functions requires to recourse to less controlled techniques for the analytic continuation of the Green functions. The second numerical method is based on Wilson's renormalization group [12,13]. This method can be formulated both at $T = 0$ and finite (small) T providing accurate results at small frequencies; thus it is very adequate for the investigation of correlated metallic phases with heavy effective-mass quasiparticles. The cost to pay is that the description of the high energy features involve approximations and cannot be so accurately obtained [14].

The goal of the present work is to introduce a new algorithm for the solution of the DMFT self-consistent equations that makes use of another powerful numerical methodology for the solution of many-body Hamiltonians: the density matrix renormalization group (DMRG) [15]. This method, like the NRG, has the appealing feature of making no *a priori* approximations and the possibility of a systematic improvement of the quality of the solutions. However, unlike NRG, it is not formulated as a low-frequency asymptotic method [14] and thus may provide equally reliable solutions for both gapless and gapfull phases. More significantly, it provides accurate estimates for the distributions of spectral intensities of high frequency features such as the Hubbard bands that are of main relevance for analysis of x-ray photoemission and optical conductivity experiments.

We shall illustrate the new formulation with the solution of the, by now classic, Mott transition in the Hubbard model. We shall show that accurate estimates of the critical interactions for the metal-to-insulator and for the insulator-to-metal transitions at $T = 0$ can be obtained, and, interestingly, we find evidence of substructure in the Hubbard bands in the correlated metallic phase.

The Hamiltonian of the Hubbard model is defined by

$$H = t \sum_{\langle i,j\rangle,\sigma} c^{\dagger}_{i,\sigma} c_{j,\sigma} + U \sum_{i} n_{i,\downarrow} n_{i,\uparrow}. \quad (1)$$

The treatment of this model with DMFT leads to a mapping of the original lattice model onto an associated quantum impurity problem in a self-consistent bath. In the particular case of the Hubbard model, the associated impurity problem is the single impurity Anderson model (SIAM), where the hybridization function $\Delta(\omega)$, which in the usual SIAM is a flat density of states of the conduction electrons, is now to be determined self-consistently. More precisely, for the Hamiltonian (1) defined on a Bethe lattice of coordination d, one takes the limit of large d and exactly maps the model onto a SIAM impurity problem with the requirement that $\Delta(\omega) = t^2 G(\omega)$, where $G(\omega)$ is the impurity Green's function. At the self-consistent point, $G(\omega)$ coincides with the *local* Green's function of the original lattice model [3]. The half-bandwidth of the noninteracting model is our energy unit, $2t = 1$.

A central quantity in this algorithm is the noninteracting Green's function of the impurity problem, $G_0(\omega) = 1/[\omega + \mu - \Delta(\omega)] = 1/[\omega + \mu - t^2 G(\omega)]$. Thus, to implement the new algorithm we shall consider [16,17] a general representation of the hybridization function in terms of continued fractions that define a parametrization of $\Delta(\omega)$ in terms of a set of real and positive coefficients. Since it is essentially a Green's function, $\Delta(z)$ can be decomposed into "particle" and "hole" contributions as $\Delta(z) = \Delta^{>}(z) + \Delta^{<}(z)$ with $\Delta^{>}(z) = t^2 \langle gs| c \frac{1}{z-(H-E_0)} c^{\dagger} |gs\rangle$ and $\Delta^{<}(z) = t^2 \langle gs| c^{\dagger} \frac{1}{z+(H-E_0)} c |gs\rangle$ for a given Hamiltonian, H, with ground-state energy, E_0. By standard Lanczos technique, H can be in principle tridiagonalized and the functions $\Delta^{>}(z)$ and $\Delta^{<}(z)$ can be expressed in terms of respective continued fractions [18]. Each continued fraction can be represented by a chain of auxiliary atomic sites whose energies and hopping amplitudes are given by the continued fraction diagonal and off-diagonal coefficients, respectively, [16,17].

From the self-consistency condition, the two chains representing the hybridization are "attached" to the right and left of an atomic site to obtain a new SIAM Hamiltonian, H. In fact, $G_0(z)$ constitutes the local Green's function of the site plus chain system.

The algorithm in Refs. [16,17] basically consists in switching on the local Coulomb interaction at the impurity site of the SIAM Hamiltonian and uses the Lanczos technique to reobtain $\Delta(z)$, iterating the procedure until the set of continued fractions coefficients converges.

A great limitation of this procedure is that the number of auxiliary atomic sites that needs to be used in the hybridization chains is too large for standard exact diagonalization schemes. Therefore, the chains have to be cut at very short lengths, and as a consequence, the method becomes approximate with sizable finite-size effects. In the present work, we shall make a fundamental improvement on this scheme, namely, diagonalizing the Hamiltonian using DMRG, which in principle allows to handle chains of arbitrary length [19].

The SIAM Hamiltonian therefore reads

$$\begin{aligned} H = & \sum_{\sigma,\alpha=-N_C,\alpha\neq 0}^{N_C} a_\alpha c^{\dagger}_{\alpha\sigma} c_{\alpha\sigma} \\ & + \sum_{\sigma,\alpha=-(N_C-1),\alpha\neq 0,-1}^{N_C-1} b_\alpha (c^{\dagger}_{\alpha\sigma} c_{\alpha+1\sigma} + \text{H.c.}) \\ & + \sum_{\sigma,\alpha=\pm 1} b_0 (c^{\dagger}_{\sigma} c_{\alpha\sigma} + \text{H.c.}) + U\left(n_\uparrow - \frac{1}{2}\right)\left(n_\downarrow - \frac{1}{2}\right), \end{aligned} \quad (2)$$

with c_σ being the destruction operator at the impurity site, and $c_{\alpha\sigma}$ being the destruction operator at the α site of the hybridization chain of $2N_C$ sites. The set of parameters $\{a_\alpha, b_\alpha\}$ are directly obtained from the coefficients of the continued fraction representations of $\Delta(z)$ by the procedure just described. An important point to make is that while the hopping to an impurity connected to a chain bears a resemblance to the NRG method, the present formulation is different in a crucial aspect: unlike NRG, it is not constructed as an asymptotically exact representation for low frequencies, but rather treats all energy scales on equal footing. By paying the price of giving up the excellent resolution at low-frequency of NRG, we shall gain in exchange a controlled and systematic algorithm operating at *all* energy scales. As in Wilson's NRG, the energy resolution depends on the length of the auxiliary chain; considering longer chains while keeping the numerical accuracy in the computation is the central limitation of the current scheme. In practice, systems of up to 45 ($N_C = 22$) sites were considered.

In Fig. 1 we show the DMFT + DMRG results (solid lines) for the density of states (DOS) for several values of increasing interaction U. The results are compared to the iterated perturbation theory (IPT) results (dashed lines) [1,20]; IPT is a useful analytic approximate method that

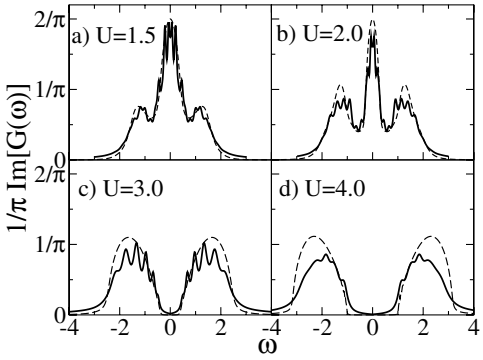

FIG. 1. Half-filled Hubbard model density of states ($\frac{1}{\pi}\text{Im}G(\omega)$) [25] pinning.

can be solved on the real frequency axis at $T = 0$. In Fig. 2 we compare the DMFT + DMRG results (solid lines) for the imaginary part of the Green's function on the imaginary frequency axis with the corresponding ones obtained by quantum Monte Carlo solution of the DMFT equations at a low temperature (circles). We see that the overall agreement on the real axis is very satisfactory and on the Matsubara frequency axis it is excellent. At low values of U, we find a metallic state characterized by a narrow quasiparticle feature at low frequencies. Increasing U, this peak gets narrower by transferring spectral weight to features at higher energies of order U, the upper and lower Hubbard bands. At large values of the interaction, the system evolves toward an insulator with a gap of order U [Fig. 3(c)].

A very important feature of the metal-insulator transition in the paramagnetic state of the Hubbard model at half filling [3] is that there are two distinct critical values of the interaction associated with the transition: U_{c1} and U_{c2}. The former signals the insulator-to-metal transition obtained upon lowering the interaction, while the latter corresponds to the metal-to-insulator transition obtained when the Fermi liquid is destroyed by increasing the interaction strength. We obtained estimates of these two values that are consistent with those from NRG calculations [12]. We find $U_{c1} = 2.39 \pm 0.02$ and $U_{c2} = 3.0 \pm 0.2$. Because of the nature of this algorithm and the arguments presented before, we expect that our determination of U_{c1} should be more accurate than NRG (and all other previously used $T = 0$ methods). Our criterion for the investigation of metallic versus insulating states was based on the behavior of the spectral weight at zero frequency and the size of the gap in the DOS (given by the energy of the first pole). It was a remarkable finding that these quantities showed an unexpected dramatic dependence with the length of the hybridization chain and the proximity to the critical value of the interaction. This dramatic effect is demonstrated in Fig. 3, where we plot the results as a function of the inverse of the chain length at $U = 2.3$ [Fig. 3(a)] and $U = 2.5$ [Fig. 3(b)]. We find that as U is increased from the weak coupling (metallic) side, chains longer than a U-dependent value L_c were required to converge to metallic solutions [Fig. 3(d)]. The value of L_c was in fact found to *diverge* at a finite interaction strength that we identified with our estimate of U_{c2}. As long as the length $L = N_c < L_c$, the solution looks as that of an insulating state with vanishing DOS at $\omega = 0$, while a rapid crossover to a metallic solution is seen as L goes beyond the threshold value L_c. This resembles the behavior of the Kondo effect in finite systems [21], where the Kondo effect is suppressed if the Kondo screening cloud is larger than the system size. This similarity also shows up in the increase of L_c with U, as in the Kondo model the correlation length increases with the interaction.

For the insulator-to-metal transition, the value of U_{c1} can be determined by the closure of the gap in the DOS or using the inverse of the second moment of the DOS [22], Fig. 3(c). Any of these two quantities are nonzero in the insulating state and vanish at U_{c1}.

Another interesting result that has been a matter of debate, and might have implications for the analysis of x-ray photoemission spectra, is the question of the existence on substructure in the Hubbard bands of the correlated metallic state. The substructure was first identified within approximate calculations [20,23], but the exact numerical methods did not have the required accuracy to decide whether the substructure was an artifact borne out of the approximations or a real feature of the model's solution. In fact, an appealing physical interpretation of the substructure can be readily made: in a rigid band picture, one can think of the action of the local interaction U to "split" and replicate the hybridization function density of states $\Delta(\omega)$ at frequencies $\pm U/2$. This in fact gives a simple qualitative understanding of the emergence of Hubbard bands in the insulator when U is large. The

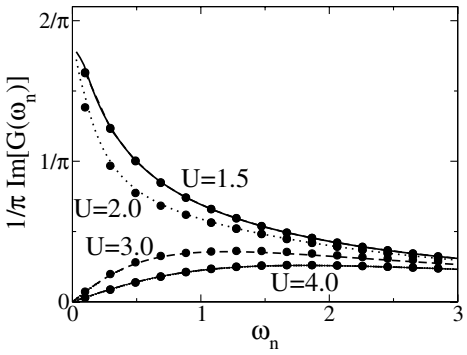

FIG. 2. Imaginary part of the Green functions at imaginary (Matsubara) frequencies (solid lines). We also show quantum Monte Carlo results (circles) at low temperature $T = 1/32$.

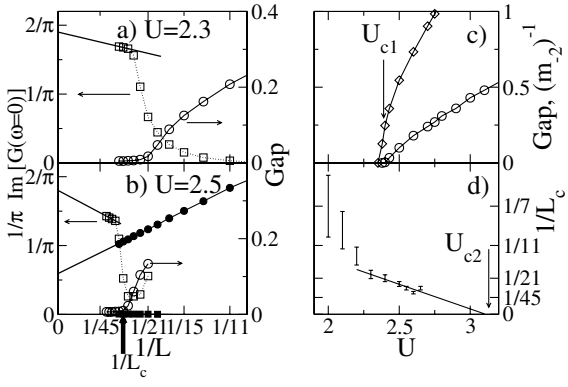

FIG. 3. DOS at the Fermi energy (squares) and gap (circles) for (a) $U = 2.3$ and (b) $U = 2.5$. Open (closed) symbols correspond to metallic (insulating) solutions. The thick arrow shows the critical length (L_c) above which a metallic solution is obtained. (c) Gap (circles) and inverse of the second moment of the DOS (diamond) as a function of U. The values correspond to extrapolations to infinite-size chains. (d) $1/L_c$ as a function of U.

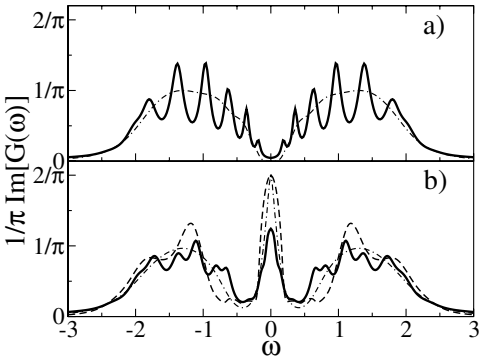

FIG. 4. Density of states for $U = 2.5$ (solid line). For comparison NRG (dot-dashed line) and IPT (dashed line) results are also shown. (a) Insulating solution. (b) Metallic solution.

semicircular $\Delta(\omega)$ is duplicated into the two (approximate) semicircles at $\pm U/2$ of the local DOS (the imaginary part of $G(\omega)$) characteristic of the Mott-Hubbard insulator. Then one realizes that the self-consistency requires $\Delta(\omega)$ to coincide with $t^2 G(\omega)$; thus, if $\mathrm{Im}[G(\omega)]$ develops (multipeak) structure, it implies that $\Delta(\omega)$ has a similar structure. Then, by the simple-minded argument in which the action of U is to "split and replicate," we get (multipeak) structures for the Hubbard bands at $\pm U/2$ in the DOS, in a self-consistent manner. In Fig. 4 we show the comparison of the DOS of the model for both the correlated metallic and insulating solutions at the same value of the interaction $U = 2.5$ (i.e., between U_{c1} and U_{c2}). The results show that the smooth envelope of the pole structure (due to a finite N_c forming the lower and upper Hubbard bands in the insulator) acquires more structure in the metallic state. For comparison, we also plot the corresponding results from NRG [24] and IPT. The former fails to capture any qualitative difference between the shape of the metallic and insulating Hubbard bands; however, IPT shows a very smooth shape for the insulator [cf. Fig. 1(c) and 1(d)] and a multipeak structure in the metallic Hubbard bands. The structure of IPT is in qualitative agreement with the spectral distribution of weight born out from the DMRG calculation. To our knowledge, this is the first strong evidence of the existence of nontrivial structure in the Hubbard bands within DMFT.

To conclude, we have presented a new algorithm to solve the DMFT equations of strongly correlated models exploiting the DMRG methodology. Large systems can be considered and accurate values of the critical interactions are obtained in agreement with NRG predictions, allowing for a nontrivial test of the accuracy of this method. In contrast with NRG, however, this new algorithm deals with all energy scales on equal footing, which allowed us to find interesting substructure in the Hubbard bands of the correlated metallic state. The ability of the new algorithm to directly deal with the high energy scales is a very important feature that is relevant for the interpretation of the high resolution photoemission spectroscopies that are becoming available from the new generation sinchrotron machines [4]. In addition, this method could also handle more general models having a larger number of degrees of freedom such as the multiorbital Hubbard models required for realistic band-structure calculations of strongly correlated systems.

We thank R. Bulla for the NRG data and B. Alascio for useful discussions. We acknowledge support from CONICET (PEI6360), Fundación Antorchas (14116-168), and ANPCyT PICT 03-06343 and 03-11609.

Note added.—During the review process we became aware of a related work by S. Nishimoto *et al.* using a different DMRG method.

[1] A. Georges and G. Kotliar, Phys. Rev. B **45**, 6479 (1992).
[2] W. Metzner and D. Vollhardt, Phys. Rev. Lett. **62**, 324 (1989).
[3] A. Georges *et al.*, Rev. Mod. Phys. **68**, 13 (1996).
[4] G. Kotliar and D. Vollhardt, Phys. Today **57**, No. 3, 53 (2004).
[5] X. Dai *et al.*, Science, **300**, 953 (2003); S. Savrasov, G. Kotliar, and E. Abrahams, Nature (London) **410**, 793 (2001).
[6] D. Vollhardt *et al.*, cond-mat/0408266.
[7] Y. Kakehashi and P. Fulde, Phys. Rev. B **32**, 1595 (1985).
[8] J. E. Hirsch and R. M. Fye, Phys. Rev. Lett. **56**, 2521 (1986).
[9] K. G. Wilson, Rev. Mod. Phys. **47**, 773 (1975).
[10] M. J. Rozenberg, Phys. Rev. B **55**, R4855 (1997).
[11] M. J. Rozenberg *et al.*, Phys. Rev. Lett. **83**, 3498 (1999).
[12] R. Bulla, Phys. Rev. Lett. **83**, 136 (1999).
[13] R. Bulla *et al.*, Phys. Rev. B **64**, 045103 (2001).
[14] C. Raas *et al.*, Phys. Rev. B **69**, 041102(R) (2004).
[15] *Density Matrix Renormalization*, Lecture Notes in Physics, edited by I. Peschel *et al.* (Springer-Verlag, Berlin, 1999); S. R. White, Phys. Rev. Lett. **69**, 2863 (1992).
[16] Q. Si *et al.*, Phys. Rev. Lett. **72**, 2761 (1994).
[17] M. J. Rozenberg *et al.*, Mod. Phys. Lett. B **8**, 535 (1994).
[18] K. Hallberg, Phys. Rev. B **52**, R9827 (1995).
[19] See, e.g., F. Gebhard *et al.*, Eur. Phys. J. B **36**, 491 (2003), for a previous attempt using a particular algorithm of the DMRG restricted to the small U metallic regime.
[20] X. Y. Zhang, M. J. Rozenberg, and G. Kotliar, Phys. Rev. Lett. **70**, 1666 (1993); Phys. Rev. B **49**, 10181 (1994); A. Georges and W. Krauth, Phys. Rev. B **48**, 7167 (1993).
[21] P. Cornaglia and C. Balseiro, Phys. Rev. Lett. **90**, 216801 (2003).
[22] M. J. Rozenberg *et al.*, Phys. Rev. B **54**, 8452 (1996).
[23] S. Florens and A. Georges, Phys. Rev. B **66**, 165111 (2002).
[24] R. Bulla (private communication).
[25] The "pinning" condition seems not to be obeyed due to the finite broadening of the δ-function poles.